

# EUROPEAN ORGANIZATION FOR NUCLEAR RESEARCH

## Proposal to the ISOLDE and Neutron Time-of-Flight Committee

(Following HIE-ISOLDE Letter of Intent I-114)

### Shape Transition and Coexistence in Neutron-Deficient Rare Earth Isotopes

[3.10.2012]

A. Gørgen<sup>1</sup>, F.L. Bello Garrote<sup>1</sup>, P.A. Butler<sup>2</sup>, J. Cederkäll<sup>3</sup>, E. Clément<sup>4</sup>, J.-P. Delaroche<sup>5</sup>,  
L. Gaffney<sup>2</sup>, M. Girod<sup>5</sup>, M.S. Guttormsen<sup>1</sup>, T.W. Hagen<sup>1</sup>, P. Hoff<sup>6</sup>, D.G. Jenkins<sup>7</sup>, J. Jolie<sup>8</sup>,  
M. Klintefjord<sup>1</sup>, W. Korten<sup>9</sup>, A.C. Larsen<sup>1</sup>, J.Ljungvall<sup>10</sup>, G. O'Neill<sup>2</sup>, P. Reiter<sup>8</sup>, E. Sahin<sup>1</sup>,  
M.-D. Salsac, S. Siem<sup>1</sup>, N. Warr<sup>8</sup>, M. Zielinska<sup>9</sup>

<sup>1</sup> Department of Physics, University of Oslo, Norway

<sup>2</sup> Oliver Lodge Laboratory, University of Liverpool, United Kingdom

<sup>3</sup> Department of Physics, Lund University, Sweden

<sup>4</sup> GANIL, Caen, France

<sup>5</sup> CEA-DIF, Bruyères-le-Châtel, France

<sup>6</sup> Department of Chemistry, University of Oslo, Norway

<sup>7</sup> Department of Physics, University of York, United Kingdom

<sup>8</sup> Institut für Kernphysik, Universität zu Köln, Germany

<sup>9</sup> CEA Saclay, IRFU/SPhN, France

<sup>10</sup> CSNSM, CNRS-IN2P3, Orsay, France

Spokesperson: Andreas Gørgen (andreas.gorgen@fys.uio.no)

Local contact: Elisa Rapisarda (Elisa.Rapisarda@cern.ch)

#### Abstract

We propose to study spectroscopic quadrupole moments of excited states and electromagnetic transition rates between them in the neutron-deficient rare earth nuclei  $^{140}\text{Sm}$  and  $^{142}\text{Gd}$  using projectile Coulomb excitation at energies of 4.7 MeV per nucleon. The rare earth nuclei below the N=82 shell closure form one of the few regions of the nuclear chart where oblate shapes are expected to occur near the ground state. Nuclear shapes are expected to change rapidly in this region, with coexistence of oblate and prolate shapes in some nuclei. The measurement of electromagnetic matrix elements represents therefore a particularly sensitive test of theoretical nuclear structure models.

**Requested shifts:** 24 shifts, split into 2 runs (12 shifts for  $^{140}\text{Sm}$  and 12 shifts for  $^{142}\text{Gd}$ )

**Beamline:** MINIBALL + CD-only



## 1. Physics case

The measurement of dynamic and static electromagnetic moments represents one of the most sensitive probes of nuclear structure and the most direct method to study nuclear collectivity and shapes. The motion of individual nucleons depends critically on the nuclear shape, and conversely the shape can be strongly influenced by a few individual nucleons. The deformation can be described by a multipole expansion, with the quadrupole deformation being the most important deviation from spherical shape. Such quadrupole shapes can either have axial symmetry, in which case one distinguishes elongated (prolate) and flattened (oblate) shapes, or the deformation can be without axial symmetry resulting in a triaxial shape. In particular for heavy nuclei with  $N, Z > 50$  a strong dominance of prolate shapes is observed, which has been related to the strength of the spin-orbit interaction relative to the radial term in the nuclear interaction [1]. Oblate shapes are then only expected when a major shell is almost filled due to the strong shape-driving effect of holes in the  $\Omega=1/2$  orbitals. In these regions of the nuclear chart the shape is very sensitive to structural effects and can change from one nucleus to its neighbor. This effect is seen for example in HFB calculations, which predict the occurrence of oblate ground-state shapes for example just below the  $N=82$ ,  $N=126$ , and  $Z=82$  shell closures (see Fig. 1).

Apart from the fundamental question where in the nuclear chart oblate shapes can be found, nuclei with oblate ground-state shapes are also the best candidates to study the phenomenon of oblate-prolate shape coexistence. In addition to changes of the nuclear shape with proton or neutron number, the shape can also change with excitation energy or angular momentum within the same nucleus. Such changes are caused by a rearrangement of the orbital configuration of the nucleons or by the dynamic response of the nuclear system to rotation. In some cases configurations corresponding to different shapes coexist at similar energies. The wave functions of such states can then mix according to the laws of quantum mechanics. Because the calculation of nuclear shapes and related observables is very sensitive to such structural effects, regions of the nuclear chart where the shape changes rapidly and shape coexistence occurs represent an ideal testing ground for theoretical models and the effective nucleon-nucleon interactions that they employ.

Some of the best example for shape coexistence are found in the region of neutron-deficient Pb and Hg isotopes, near the  $Z=82$  proton shell closure and in the mid-shell region for neutrons. The present proposal addresses nuclei below the  $N=82$  neutron shell closure near the mid-shell region for protons. Exchanging the role of protons and neutrons, similar shape phenomena can be expected in both regions. Theoretical calculations predict the occurrence of oblate deformed shapes near the ground state and oblate-prolate shape coexistence in particular for the  $N=78$  isotones with  $Z > 60$ . The experimental observables most closely related to the nuclear shape are quadrupole moments of excited states and electromagnetic transition rates between them. These observables are accessible in Coulomb excitation experiments.

## 2. Present experimental knowledge

The neutron-deficient rare earth nuclei are accessible via heavy-ion induced fusion-evaporation reactions. Some of them, e.g.  $^{142}\text{Gd}$  [2,3], have been studied in great detail up to high spins. However, experimental studies of the shapes near the ground state are lacking completely for these nuclei. The yrast cascades for the  $N=78$  isotones up to  $^{144}\text{Dy}$  are known from fusion-evaporation experiments; non-yrast states have been observed in  $\beta$ -decay studies up to  $^{142}\text{Gd}$ . As an example, the known level scheme for  $^{142}\text{Gd}$  is shown in Fig.2. The  $B(E2)$  values between low-lying states are unknown because the occurrence of long-lived  $10^+$  states hampers lifetime measurements below these isomers. Coulomb excitation is therefore the method of choice to measure  $B(E2)$  values between low-lying states, which furthermore gives access to spectroscopic

quadrupole moments via the reorientation effect and hence allows a direct measurement of the nuclear shape associated with a specific state.

In  $^{140}\text{Sm}$  a state at 990 keV excitation energy has been tentatively assigned as an excited  $0^+$  state [4]. If this assignment is correct, this low-lying  $0^+$  state could be interpreted as a sign of shape coexistence. The structure of the non-yrast states in  $^{142}\text{Gd}$  is unclear.

### 3. Theoretical predictions

The HFB calculations with Gogny D1S interaction shown in Fig.1 predict strongly deformed prolate shapes in the deformed region above  $Z=50$  and below  $N=82$ , except for a small region of oblate shapes for the most proton-rich  $N=78$  and  $N=76$  isotones. Relativistic mean-field (RMF) calculations with the NL-SH parameterization of the RMF Lagrangian find similar ground-state shapes for the most proton-rich  $N=78$  isotones [5].

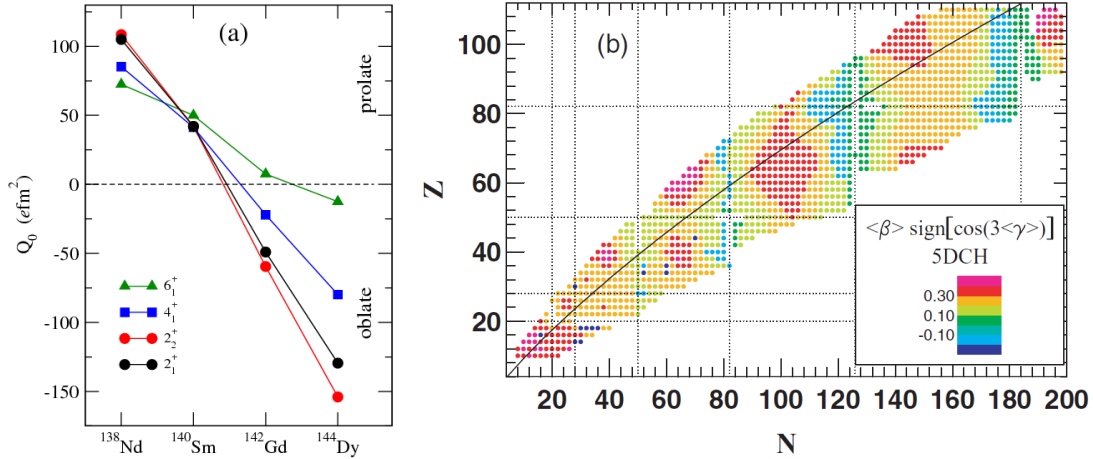


Fig 1: (a) Intrinsic quadrupole moments for excited states in even-even nuclei with  $N=78$  and  $60 \leq Z \leq 66$  from beyond-mean-field calculations with the Gogny D1S force. (b) Nuclear chart showing predictions for the ground-state deformation [6].

The rapid shape transition predicted by the different mean-field calculations suggests that shape coexistence may be found in the transitional region. To account for configuration mixing, correlations beyond the mean field have to be considered in the calculations. Significant progress has been achieved in recent years in the description of collective nuclear excitations in models which include such correlations. Configuration mixing can be described by introducing fluctuations in the collective degrees of freedom with the so-called Generator Coordinate Method (GCM). We have performed HFB-based configuration mixing calculations using the Gogny D1S interaction and the GCM approach with Gaussian overlap approximation comprising axial and non-axial quadrupole deformations [6] to investigate the sensitivity of the model to the shape effects described above.

The calculations reproduce the experimentally known excitation energies well. As an example, the calculated and experimental level schemes are compared for  $^{142}\text{Gd}$  in Fig.2. Experimental spin and parity assignments are only known for the ground-state rotational band, and no transition strengths are experimentally known between the low-lying states. In the calculation the low-lying states can be grouped into three bands (only states with positive parity are calculated): the ground-state band, a  $\gamma$ -vibrational band, and a band based on an excited  $0^+$  state with larger deformation of opposite sign compared to the ground-state band. The collectivity is increasing slowly with proton number  $Z$  and rapidly with decreasing neutron number  $N$ . The most interesting result concerns the sign of the quadrupole moments: Along the

chain of  $N=78$  isotones the sign of the quadrupole moments changes from  $Z=62$  to  $Z=64$  (see Fig.1). The signs are consistent with prolate ground-state and  $\gamma$  bands in  $^{138}\text{Nd}$  and  $^{140}\text{Sm}$ , and oblate ground-state and  $\gamma$  bands in  $^{142}\text{Gd}$  and  $^{144}\text{Dy}$ . While  $\gamma$  vibrations are among the most commonly encountered excitation modes in deformed nuclei, there exists to our knowledge no direct evidence for  $\gamma$ -vibrational bands built on oblate shapes. Calculated  $B(E2)$  values and quadrupole moments are presented in Table 1. Note that the  $2_2^+$  states are found with predominant  $K=2$  character, resulting in opposite sign of  $Q_s(2_2^+)$  compared to  $Q_s(2_1^+)$ , even though the intrinsic shape is the same. The change of signs from  $^{140}\text{Sm}$  to  $^{142}\text{Gd}$ , on the other hand, reflects a change of the intrinsic shape. The last column of Table 1 shows the spectroscopic quadrupole moments extracted from the theoretical  $B(E2)$  values using the relation between  $B(E2)$  and  $Q_s$  of the rotational model. As can be seen, the quadrupole moments are significantly smaller than the rotational values, in particular for  $^{140}\text{Sm}$  and  $^{142}\text{Gd}$ , for which the mixing of prolate and oblate configurations is expected to be strongest.

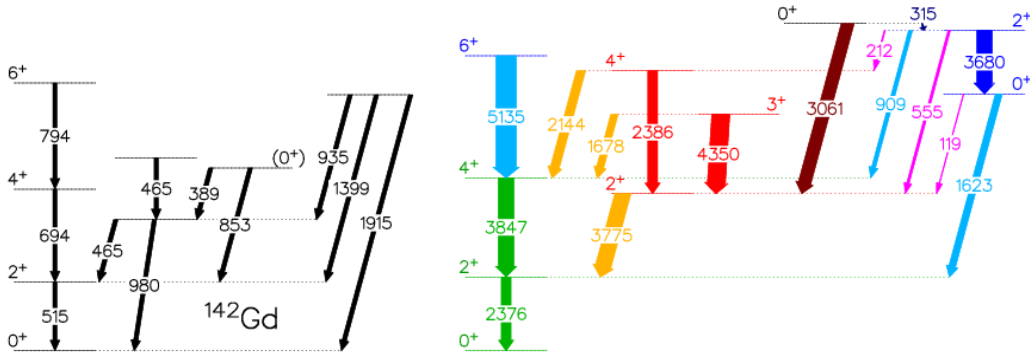


Fig 2: Left: Experimental level scheme for  $^{142}\text{Gd}$ . The transitions are labelled with their transition energy in keV. Right: Calculated level scheme using the GCM-GOA approach with the Gogny D1S interaction. The transitions are labelled with their  $B(E2)$  values in  $e^2\text{fm}^4$ . States of oblate shape are shown in green, prolate shapes in blue, and gamma-vibrational states in red. Transitions connecting states of different character are shown in the corresponding mixed colour.

	$B(E2; 2_1^+ \rightarrow 0_1^+)$ [ $e^2\text{fm}^4$ ]	$B(E2; 4_1^+ \rightarrow 2_1^+)$ [ $e^2\text{fm}^4$ ]	$Q_s(2_1^+)$ [ $\text{efm}^2$ ]	$Q_s(2_2^+)$ [ $\text{efm}^2$ ]	$Q_s(4_1^+)$ [ $\text{efm}^2$ ]	$Q_{\text{RM}}(2_1^+)$ [ $\text{efm}^2$ ]
$^{138}\text{Nd}$	1736	2853	-30	+31	-31	$\pm 84$
$^{140}\text{Sm}$	2055	3344	-12	+12	-15	$\pm 92$
$^{142}\text{Gd}$	2376	3847	14	-17	8	$\pm 99$
$^{144}\text{Dy}$	2743	4476	37	-44	29	$\pm 106$

Table 1.  $B(E2)$  values and spectroscopic quadrupole moments from the configuration-mixing calculations with Gogny D1S interaction. The last column shows the spectroscopic quadrupole moment of the  $2_1^+$  states calculated from the  $B(E2)$  values using the rotational model.

One would expect to observe low-lying  $0^+$  states, such as the one tentatively assigned in  $^{140}\text{Sm}$  [4], in the nuclei near the predicted shape transition. The calculations find the lowest  $0^+$  states at excitation energies of about 2 MeV. However, there are examples also in other mass regions where the GCM-GOA calculations have overestimated the excitation energies of  $0^+$  states. To investigate the character of the 990 keV state in  $^{140}\text{Sm}$  and to search for low-lying  $0^+$  states in neighboring nuclei is therefore of importance. If  $0^+$  states indeed exist at such low excitation energies, Coulomb excitation experiments will be able to populate and identify them.

#### 4. Preliminary results from Coulomb excitation of $^{140}\text{Sm}$ (IS495)

A first Coulomb excitation experiment in this mass region was performed at ISOLDE in the summer of 2012 using a  $^{140}\text{Sm}$  beam of  $2.84\text{-}A$  MeV energy incident on a  $^{94}\text{Mo}$  target. The beam intensity of approximately  $5\cdot 10^5$  ions per second in Miniball fully met expectations and the use of the RILIS source together with a new  $\text{GdB}_6$  cavity suppressed all isobaric contaminants. Preliminary spectra from a first analysis of the data, which were collected over four days, are shown in Fig.3. At least three excited states in  $^{140}\text{Sm}$  were populated in the experiment: the first  $2^+$  and  $4^+$  states and the tentatively assigned  $0^+$  state at 990 keV excitation energy, which decays via a 460 keV transition to the first  $2^+$  state. The population of both the  $4^+$  and the presumed  $0^+$  state require two-step excitation. It is expected that further analysis of the data will yield the presently unknown  $B(E2)$  values for the  $2_1^+ \rightarrow 0_1^+$ ,  $4_1^+ \rightarrow 2_1^+$ , and  $(0_2^+) \rightarrow 2_1^+$  transitions and in addition the spectroscopic quadrupole moment of the  $2^+$  state. While these quantities are very valuable to benchmark theoretical calculations, they are alone not yet enough to firmly proof the proposed shape coexistence scenario. In order to provide solid proof it would be necessary to measure the quadrupole moment of the second  $2^+$  state that is built upon the excited  $0^+$  state.

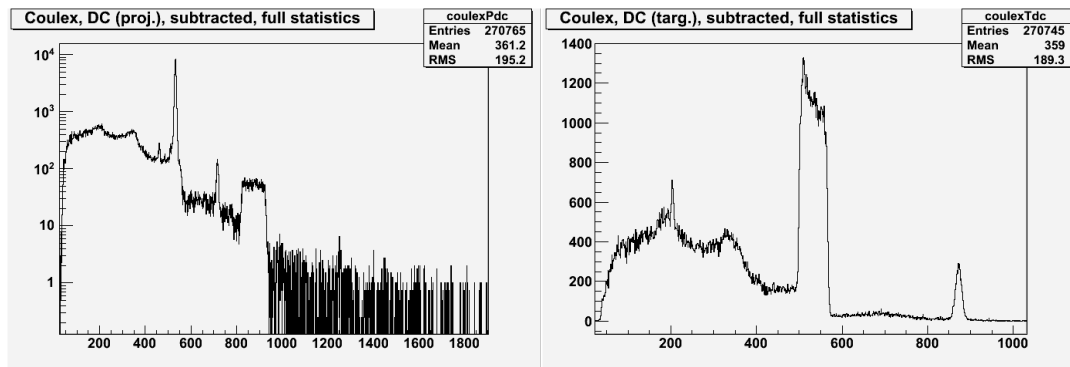


Fig 3: Preliminary gamma-ray spectra following the Coulomb excitation of  $^{140}\text{Sm}$  at  $2.84\text{-}A$  MeV on a  $^{94}\text{Mo}$  target from IS495. The spectrum on the left is Doppler corrected for the velocity vector of the projectile and shows the de-excitation of the  $2_1^+$ ,  $4_1^+$ , and  $(0_2^+)$  states; the spectrum on the right is Doppler corrected for the velocity vector of the recoiling target and shown the de-excitation of the  $2_1^+$  state in  $^{94}\text{Mo}$  that is used for normalization.

#### 5. Goals of the proposed experiment and feasibility

We propose to extend the previous study of nuclear shapes in the  $N=78$  isotones in two aspects: (i) a more comprehensive investigation of  $B(E2)$  values and quadrupole moments in  $^{140}\text{Sm}$ , which will become feasible due to the considerably higher cross sections at the higher beam energies provided by the new post-accelerator of HIE-ISOLDE and (ii) the extension of the study to neighbouring  $^{142}\text{Gd}$ , for which an inversion of the ground-state shape is predicted. To illustrate the increase in cross section with beam energy we have performed Coulomb excitation calculations for a  $^{142}\text{Gd}$  beam of  $2.90\text{-}A$  and  $4.72\text{-}A$  MeV energy, respectively, incident on a  $^{208}\text{Pb}$  target. The results are shown in Fig.4. The higher beam energy is the maximum at which influences of the nuclear force can still be excluded. It should be noted that the cross sections are based on the theoretically predicted matrix elements and that experimental values might deviate. Nevertheless, the simulations clearly show the limitations imposed by the low beam energies of the present REX accelerator.

With reasonable assumptions for the transitional matrix elements in  $^{140}\text{Sm}$ , we expect to populate at least the  $6_1^+$  and  $2_2^+$  states in addition to those observed in IS495. With a second data set obtained with a different target,  $^{208}\text{Pb}$  instead of  $^{94}\text{Mo}$ , we can utilize not only the angular

dependence, but also the  $Z$  dependence of the Coulomb excitation cross section in order to determine the spectroscopic quadrupole moments of the  $4_1^+$  and  $2_2^+$  states. In combination with the data obtained in IS495, the new experiment will hence allow studying the evolution of the nuclear shape along the ground-state band as well as possible shape coexistence between the  $2_1^+$  and  $2_2^+$  states in  $^{140}\text{Sm}$ . With cross sections estimated as described above, and assuming the same beam intensity as in IS495,  $5 \cdot 10^5$  pps, we estimate that 12 shifts of beam time are needed to achieve the goals and to complete the study of nuclear shapes in  $^{140}\text{Sm}$ .

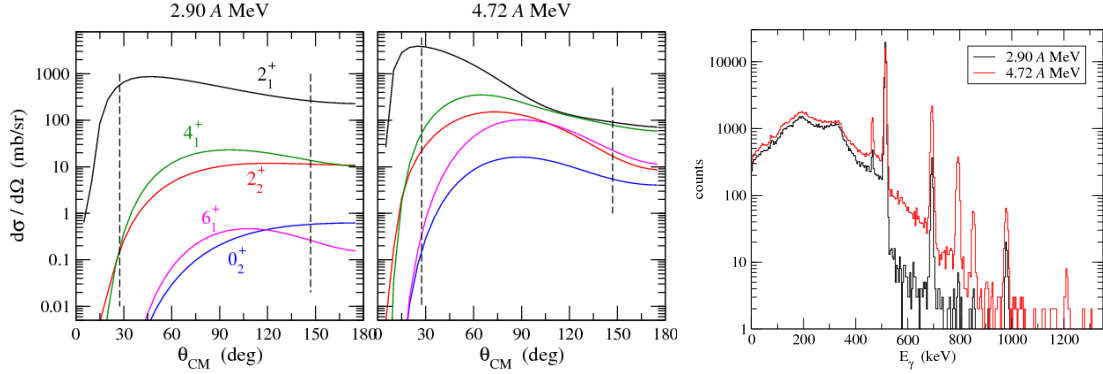


Fig 4: Comparison of cross sections to populate low-lying states in  $^{142}\text{Gd}$  by projectile Coulomb excitation on a  $^{208}\text{Pb}$  target at 2.90 and 4.72 A MeV using experimental excitation energies and matrix elements from the Gogny calculations. The vertical lines indicate the angular range covered by the setup. The cross sections were used to simulate  $\gamma$ -ray spectra for Coulomb excitation of  $^{142}\text{Gd}$  on  $^{208}\text{Pb}$  at the two beam energies, assuming an intensity of  $2.5 \cdot 10^4$  ions per second and a measuring time of four days.

In the second part of the experiment we propose to study the Coulomb excitation of  $^{142}\text{Gd}$  on a  $^{208}\text{Pb}$  target at 4.7 A MeV. The main focus will be on measuring the quadrupole moment for the  $2_1^+$  state, which is predicted to have the opposite (oblate) sign compared to  $^{140}\text{Sm}$ . At the same time the experiment will yield  $B(E2)$  values for transitions within the ground-state band and to the  $2_2^+$  state. A laser ionization scheme for Gadolinium is presently under development at ISOLDE, but has not yet been fully tested. As a conservative estimate, we assume that the beam intensity for  $^{142}\text{Gd}$  will be a factor of 20 lower than for  $^{140}\text{Sm}$ , which reflects the greater neutron deficiency, higher ionization potential, and lower volatility for  $^{142}\text{Gd}$ . Compared to the  $^{140}\text{Sm}$  experiment IS495, the lower intensity of the  $^{142}\text{Gd}$  beam will be compensated by the higher cross sections due to the increased beam energy, so the population of excited states should be comparable to the one observed for  $^{140}\text{Sm}$  in IS495. With the cross sections shown in Fig.4 and a beam intensity of  $2.5 \cdot 10^4$  pps we estimate that 12 shifts of beam time are needed to perform the measurement for  $^{142}\text{Gd}$ .

## References:

- [1] Naoki Tajima and Norifumi Suzuki, Phys. Rev. C 64, 037301 (2001).
- [2] A.A. Pasternak et al., Eur.Phys.J. A 23, 191 (2005).
- [3] E.O. Lieder et al., Eur. Phys. J. A 35, 135 (2008).
- [4] R.B. Firestone et al., Phys.Rev. C43, 1066 (1991).
- [5] G.A. Lalazissis, M.M. Sharma, P. Ring, Nucl. Phys. A 597, 35 (1996).
- [6] J.-P. Delaroche et al., Phys. Rev. C 81, 014303 (2010).

## Appendix

### DESCRIPTION OF THE PROPOSED EXPERIMENT

The experimental setup comprises: *MINIBALL + CD*

Part of the Choose an item.	Availability	Design and manufacturing
MINIBALL + CD	<input checked="" type="checkbox"/> Existing	<input checked="" type="checkbox"/> To be used without any modification
[Part 1 of experiment/ equipment]	<input type="checkbox"/> Existing	<input type="checkbox"/> To be used without any modification <input type="checkbox"/> To be modified
	<input type="checkbox"/> New	<input type="checkbox"/> Standard equipment supplied by a manufacturer <input type="checkbox"/> CERN/collaboration responsible for the design and/or manufacturing
[Part 2 experiment/ equipment]	<input type="checkbox"/> Existing	<input type="checkbox"/> To be used without any modification <input type="checkbox"/> To be modified
	<input type="checkbox"/> New	<input type="checkbox"/> Standard equipment supplied by a manufacturer <input type="checkbox"/> CERN/collaboration responsible for the design and/or manufacturing
[insert lines if needed]		

### HAZARDS GENERATED BY THE EXPERIMENT

Hazards named in the document relevant for the fixed [MINIBALL + only CD installation.

Additional hazards:

Hazards			
	[Part 1 of the experiment/equipment]	[Part 2 of the experiment/equipment]	[Part 3 of the experiment/equipment]
<b>Thermodynamic and fluidic</b>			
Pressure	[pressure][Bar], [volume][l]		
Vacuum			
Temperature	[temperature] [K]		
Heat transfer			
Thermal properties of materials			
Cryogenic fluid	[fluid], [pressure][Bar], [volume][l]		
<b>Electrical and electromagnetic</b>			
Electricity	[voltage] [V], [current][A]		
Static electricity			
Magnetic field	[magnetic field] [T]		
Batteries	<input type="checkbox"/>		
Capacitors	<input type="checkbox"/>		
<b>Ionizing radiation</b>			
Target material	208Pb		
Beam particle type (e, p, ions, etc)	140Sm	142G	
Beam intensity	5 x 10e5	2.5 x 10e4	
Beam energy	4.7 MeV/u	4.7 MeV/u	
Cooling liquids	LN2		
Gases	[gas]		
Calibration sources:	<input type="checkbox"/>		
• Open source	<input type="checkbox"/>		
• Sealed source	<input type="checkbox"/> [ISO standard]		
• Isotope	152Eu, 133Ba	152Eu, 133Ba	

• Activity	standard Miniball sources		
Use of activated material:			
• Description	<input type="checkbox"/>		
• Dose rate on contact and in 10 cm distance	[dose][mSV]		
• Isotope			
• Activity	< 10 µCi		
<b>Non-ionizing radiation</b>			
Laser	RILIS	RILIS	
UV light			
Microwaves (300MHz-30 GHz)			
Radiofrequency (1-300MHz)			
<b>Chemical</b>			
Toxic	[chemical agent], [quantity]		
Harmful	[chemical agent], [quantity]		
CMR (carcinogens, mutagens and substances toxic to reproduction)	[chemical agent], [quantity]		
Corrosive	[chemical agent], [quantity]		
Irritant	[chemical agent], [quantity]		
Flammable	[chemical agent], [quantity]		
Oxidizing	[chemical agent], [quantity]		
Explosiveness	[chemical agent], [quantity]		
Asphyxiant	[chemical agent], [quantity]		
Dangerous for the environment	[chemical agent], [quantity]		
<b>Mechanical</b>			
Physical impact or mechanical energy (moving parts)	[location]		
Mechanical properties (Sharp, rough, slippery)	[location]		
Vibration	[location]		
Vehicles and Means of Transport	[location]		
<b>Noise</b>			
Frequency	[frequency],[Hz]		
Intensity			
<b>Physical</b>			
Confined spaces	[location]		
High workplaces	[location]		
Access to high workplaces	[location]		
Obstructions in passageways	[location]		
Manual handling	[location]		
Poor ergonomics	[location]		

### 0.1 Hazard identification

3.2 Average electrical power requirements (excluding fixed ISOLDE-installation mentioned above):  
*(make a rough estimate of the total power consumption of the additional equipment used in the experiment)*

... kW